

Search for B^0 Decays to Invisible Final States and to $\nu\bar{\nu}\gamma$

B. Aubert,¹ R. Barate,¹ D. Boutigny,¹ F. Couderc,¹ J.-M. Gaillard,¹ A. Hicheur,¹ Y. Karyotakis,¹ J. P. Lees,¹ V. Tisserand,¹ A. Zghiche,¹ A. Palano,² A. Pompili,² J. C. Chen,³ N. D. Qi,³ G. Rong,³ P. Wang,³ Y. S. Zhu,³ G. Eigen,⁴ I. Ofte,⁴ B. Stugu,⁴ G. S. Abrams,⁵ A. W. Borgland,⁵ A. B. Breon,⁵ D. N. Brown,⁵ J. Button-Shafer,⁵ R. N. Cahn,⁵ E. Charles,⁵ C. T. Day,⁵ M. S. Gill,⁵ A. V. Gritsan,⁵ Y. Groysman,⁵ R. G. Jacobsen,⁵ R. W. Kadel,⁵ J. Kadyk,⁵ L. T. Kerth,⁵ Yu. G. Kolomensky,⁵ G. Kukartsev,⁵ G. Lynch,⁵ L. M. Mir,⁵ P. J. Oddone,⁵ T. J. Orimoto,⁵ M. Pripstein,⁵ N. A. Roe,⁵ M. T. Ronan,⁵ V. G. Shelkov,⁵ W. A. Wenzel,⁵ M. Barrett,⁶ K. E. Ford,⁶ T. J. Harrison,⁶ A. J. Hart,⁶ C. M. Hawkes,⁶ S. E. Morgan,⁶ A. T. Watson,⁶ M. Fritsch,⁷ K. Goetzen,⁷ T. Held,⁷ H. Koch,⁷ B. Lewandowski,⁷ M. Pelizaeus,⁷ M. Steinke,⁷ J. T. Boyd,⁸ N. Chevalier,⁸ W. N. Cottingham,⁸ M. P. Kelly,⁸ T. E. Latham,⁸ F. F. Wilson,⁸ T. Cuhadar-Donszelmann,⁹ C. Hearty,⁹ N. S. Knecht,⁹ T. S. Mattison,⁹ J. A. McKenna,⁹ D. Thiessen,⁹ A. Khan,¹⁰ P. Kyberd,¹⁰ L. Teodorescu,¹⁰ V. E. Blinov,¹¹ V. P. Druzhinin,¹¹ V. B. Golubev,¹¹ V. N. Ivanchenko,¹¹ E. A. Kravchenko,¹¹ A. P. Onuchin,¹¹ S. I. Serednyakov,¹¹ Yu. I. Skovpen,¹¹ E. P. Solodov,¹¹ A. N. Yushkov,¹¹ D. Best,¹² M. Bruinsma,¹² M. Chao,¹² I. Eschrich,¹² D. Kirkby,¹² A. J. Lankford,¹² M. Mandelkern,¹² R. K. Mommsen,¹² W. Roethel,¹² D. P. Stoker,¹² C. Buchanan,¹³ B. L. Hartfiel,¹³ S. D. Foulkes,¹⁴ J. W. Gary,¹⁴ B. C. Shen,¹⁴ K. Wang,¹⁴ D. del Re,¹⁵ H. K. Hadavand,¹⁵ E. J. Hill,¹⁵ D. B. MacFarlane,¹⁵ H. P. Paar,¹⁵ Sh. Rahatlou,¹⁵ V. Sharma,¹⁵ J. W. Berryhill,¹⁶ C. Campagnari,¹⁶ B. Dahmes,¹⁶ S. L. Levy,¹⁶ O. Long,¹⁶ A. Lu,¹⁶ M. A. Mazur,¹⁶ J. D. Richman,¹⁶ W. Verkerke,¹⁶ T. W. Beck,¹⁷ A. M. Eisner,¹⁷ C. A. Heusch,¹⁷ W. S. Lockman,¹⁷ T. Schalk,¹⁷ R. E. Schmitz,¹⁷ B. A. Schumm,¹⁷ A. Seiden,¹⁷ P. Spradlin,¹⁷ D. C. Williams,¹⁷ M. G. Wilson,¹⁷ J. Albert,¹⁸ E. Chen,¹⁸ G. P. Dubois-Felsmann,¹⁸ A. Dvoretzki,¹⁸ D. G. Hitlin,¹⁸ I. Narsky,¹⁸ T. Piatenko,¹⁸ F. C. Porter,¹⁸ A. Ryd,¹⁸ A. Samuel,¹⁸ S. Yang,¹⁸ S. Jayatilleke,¹⁹ G. Mancinelli,¹⁹ B. T. Meadows,¹⁹ M. D. Sokoloff,¹⁹ T. Abe,²⁰ F. Blanc,²⁰ P. Bloom,²⁰ S. Chen,²⁰ W. T. Ford,²⁰ U. Nauenberg,²⁰ A. Olivas,²⁰ P. Rankin,²⁰ J. G. Smith,²⁰ J. Zhang,²⁰ L. Zhang,²⁰ A. Chen,²¹ J. L. Harton,²¹ A. Soffer,²¹ W. H. Toki,²¹ R. J. Wilson,²¹ Q. L. Zeng,²¹ D. Altenburg,²² T. Brandt,²² J. Brose,²² M. Dickopp,²² E. Feltresi,²² A. Hauke,²² H. M. Lacker,²² R. Müller-Pfefferkorn,²² R. Nogowski,²² S. Otto,²² A. Petzold,²² J. Schubert,²² K. R. Schubert,²² R. Schwierz,²² B. Spaan,²² J. E. Sundermann,²² D. Bernard,²³ G. R. Bonneaud,²³ F. Brochard,²³ P. Grenier,²³ S. Schrenk,²³ Ch. Thiebaut,²³ G. Vasileiadis,²³ M. Verderi,²³ D. J. Bard,²⁴ P. J. Clark,²⁴ D. Lavin,²⁴ F. Muheim,²⁴ S. Playfer,²⁴ Y. Xie,²⁴ M. Andreotti,²⁵ V. Azzolini,²⁵ D. Bettoni,²⁵ C. Bozzi,²⁵ R. Calabrese,²⁵ G. Cibinetto,²⁵ E. Luppi,²⁵ M. Negrini,²⁵ L. Piemontese,²⁵ A. Sarti,²⁵ E. Treadwell,²⁶ R. Baldini-Ferroli,²⁷ A. Calcaterra,²⁷ R. de Sangro,²⁷ G. Finocchiaro,²⁷ P. Patteri,²⁷ M. Piccolo,²⁷ A. Zallo,²⁷ A. Buzzo,²⁸ R. Capra,²⁸ R. Contri,²⁸ G. Crosetti,²⁸ M. Lo Vetere,²⁸ M. Macri,²⁸ M. R. Monge,²⁸ S. Passaggio,²⁸ C. Patrignani,²⁸ E. Robutti,²⁸ A. Santroni,²⁸ S. Tosi,²⁸ S. Bailey,²⁹ G. Brandenburg,²⁹ M. Morii,²⁹ E. Won,²⁹ R. S. Dubitzky,³⁰ U. Langenegger,³⁰ W. Bhimji,³¹ D. A. Bowerman,³¹ P. D. Dauncey,³¹ U. Egede,³¹ J. R. Gaillard,³¹ G. W. Morton,³¹ J. A. Nash,³¹ G. P. Taylor,³¹ M. J. Charles,³² G. J. Grenier,³² U. Mallik,³² J. Cochran,³³ H. B. Crawley,³³ J. Lamsa,³³ W. T. Meyer,³³ S. Prell,³³ E. I. Rosenberg,³³ J. Yi,³³ M. Davier,³⁴ G. Grosdidier,³⁴ A. Höcker,³⁴ S. Laplace,³⁴ F. Le Diberder,³⁴ V. Lepeltier,³⁴ A. M. Lutz,³⁴ T. C. Petersen,³⁴ S. Plaszczynski,³⁴ M. H. Schune,³⁴ L. Tantot,³⁴ G. Wormser,³⁴ C. H. Cheng,³⁵ D. J. Lange,³⁵ M. C. Simani,³⁵ D. M. Wright,³⁵ A. J. Bevan,³⁶ C. A. Chavez,³⁶ J. P. Coleman,³⁶ I. J. Forster,³⁶ J. R. Fry,³⁶ E. Gabathuler,³⁶ R. Gamet,³⁶ R. J. Parry,³⁶ D. J. Payne,³⁶ R. J. Sloane,³⁶ C. Touramanis,³⁶ J. J. Back,³⁷ C. M. Cormack,³⁷ P. F. Harrison,³⁷ * F. Di Lodovico,³⁷ G. B. Mohanty,³⁷ C. L. Brown,³⁸ G. Cowan,³⁸ R. L. Flack,³⁸ H. U. Flaecher,³⁸ M. G. Green,³⁸ P. S. Jackson,³⁸ T. R. McMahon,³⁸ S. Ricciardi,³⁸ F. Salvatore,³⁸ M. A. Winter,³⁸ D. Brown,³⁹ C. L. Davis,³⁹ J. Allison,⁴⁰ N. R. Barlow,⁴⁰ R. J. Barlow,⁴⁰ P. A. Hart,⁴⁰ M. C. Hodgkinson,⁴⁰ G. D. Lafferty,⁴⁰ A. J. Lyon,⁴⁰ J. C. Williams,⁴⁰ A. Farbin,⁴¹ W. D. Hulsbergen,⁴¹ A. Jawahery,⁴¹ D. Kovalskyi,⁴¹ C. K. Lae,⁴¹ V. Lillard,⁴¹ D. A. Roberts,⁴¹ G. Blaylock,⁴² C. Dallapiccola,⁴² K. T. Flood,⁴² S. S. Hertzbach,⁴² R. Kofler,⁴² V. B. Koptchev,⁴² T. B. Moore,⁴² S. Saremi,⁴² H. Staengle,⁴² S. Willocq,⁴² R. Cowan,⁴³ G. Sciolla,⁴³ F. Taylor,⁴³ R. K. Yamamoto,⁴³ D. J. J. Mangeol,⁴⁴ P. M. Patel,⁴⁴ S. H. Robertson,⁴⁴ A. Lazzaro,⁴⁵ F. Palombo,⁴⁵ J. M. Bauer,⁴⁶ L. Cremaldi,⁴⁶ V. Eschenburg,⁴⁶ R. Godang,⁴⁶ R. Kroeger,⁴⁶ J. Reidy,⁴⁶ D. A. Sanders,⁴⁶ D. J. Summers,⁴⁶ H. W. Zhao,⁴⁶ S. Brunet,⁴⁷ D. Côté,⁴⁷ P. Taras,⁴⁷ H. Nicholson,⁴⁸ N. Cavallo,⁴⁹ F. Fabozzi,⁴⁹ † C. Gatto,⁴⁹ L. Lista,⁴⁹ D. Monorchio,⁴⁹ P. Paolucci,⁴⁹ D. Piccolo,⁴⁹ C. Sciacca,⁴⁹ M. Baak,⁵⁰ H. Bulten,⁵⁰

G. Raven,⁵⁰ L. Wilden,⁵⁰ C. P. Jessop,⁵¹ J. M. LoSecco,⁵¹ T. A. Gabriel,⁵² T. Allmendinger,⁵³ B. Brau,⁵³ K. K. Gan,⁵³ K. Honscheid,⁵³ D. Hufnagel,⁵³ H. Kagan,⁵³ R. Kass,⁵³ T. Pulliam,⁵³ A. M. Rahimi,⁵³ R. Ter-Antonyan,⁵³ Q. K. Wong,⁵³ J. Brau,⁵⁴ R. Frey,⁵⁴ O. Igonkina,⁵⁴ C. T. Potter,⁵⁴ N. B. Sinev,⁵⁴ D. Strom,⁵⁴ E. Torrence,⁵⁴ F. Colecchia,⁵⁵ A. Dorigo,⁵⁵ F. Galeazzi,⁵⁵ M. Margoni,⁵⁵ M. Morandin,⁵⁵ M. Posocco,⁵⁵ M. Rotondo,⁵⁵ F. Simonetto,⁵⁵ R. Stroili,⁵⁵ G. Tiozzo,⁵⁵ C. Voci,⁵⁵ M. Benayoun,⁵⁶ H. Briand,⁵⁶ J. Chauveau,⁵⁶ P. David,⁵⁶ Ch. de la Vaissière,⁵⁶ L. Del Buono,⁵⁶ O. Hamon,⁵⁶ M. J. J. John,⁵⁶ Ph. Leruste,⁵⁶ J. Malcles,⁵⁶ J. Ocariz,⁵⁶ M. Pivk,⁵⁶ L. Roos,⁵⁶ S. T'Jampens,⁵⁶ G. Therin,⁵⁶ P. F. Manfredi,⁵⁷ V. Re,⁵⁷ P. K. Behera,⁵⁸ L. Gladney,⁵⁸ Q. H. Guo,⁵⁸ J. Panetta,⁵⁸ F. Anulli,^{27,59} M. Biasini,⁵⁹ I. M. Peruzzi,^{27,59} M. Pioppi,⁵⁹ C. Angelini,⁶⁰ G. Batignani,⁶⁰ S. Bettarini,⁶⁰ M. Bondioli,⁶⁰ F. Bucci,⁶⁰ G. Calderini,⁶⁰ M. Carpinelli,⁶⁰ V. Del Gamba,⁶⁰ F. Forti,⁶⁰ M. A. Giorgi,⁶⁰ A. Lusiani,⁶⁰ G. Marchiori,⁶⁰ F. Martinez-Vidal,^{60,‡} M. Morganti,⁶⁰ N. Neri,⁶⁰ E. Paoloni,⁶⁰ M. Rama,⁶⁰ G. Rizzo,⁶⁰ F. Sandrelli,⁶⁰ J. Walsh,⁶⁰ M. Haire,⁶¹ D. Judd,⁶¹ K. Paick,⁶¹ D. E. Wagoner,⁶¹ N. Danielson,⁶² P. Elmer,⁶² Y. P. Lau,⁶² C. Lu,⁶² V. Miftakov,⁶² J. Olsen,⁶² A. J. S. Smith,⁶² A. V. Telnov,⁶² F. Bellini,⁶³ G. Cavoto,^{62,63} R. Faccini,⁶³ F. Ferrarotto,⁶³ F. Ferroni,⁶³ M. Gaspero,⁶³ L. Li Gioi,⁶³ M. A. Mazzoni,⁶³ S. Morganti,⁶³ M. Pierini,⁶³ G. Piredda,⁶³ F. Safai Tehrani,⁶³ C. Voena,⁶³ S. Christ,⁶⁴ G. Wagner,⁶⁴ R. Waldi,⁶⁴ T. Adye,⁶⁵ N. De Groot,⁶⁵ B. Franek,⁶⁵ N. I. Geddes,⁶⁵ G. P. Gopal,⁶⁵ E. O. Olaiya,⁶⁵ R. Aleksan,⁶⁶ S. Emery,⁶⁶ A. Gaidot,⁶⁶ S. F. Ganzhur,⁶⁶ P.-F. Giraud,⁶⁶ G. Hamel de Monchenault,⁶⁶ W. Kozanecki,⁶⁶ M. Langer,⁶⁶ M. Legendre,⁶⁶ G. W. London,⁶⁶ B. Mayer,⁶⁶ G. Schott,⁶⁶ G. Vasseur,⁶⁶ Ch. Yèche,⁶⁶ M. Zito,⁶⁶ M. V. Purohit,⁶⁷ A. W. Weidemann,⁶⁷ J. R. Wilson,⁶⁷ F. X. Yumiceva,⁶⁷ D. Aston,⁶⁸ R. Bartoldus,⁶⁸ N. Berger,⁶⁸ A. M. Boyarski,⁶⁸ O. L. Buchmueller,⁶⁸ M. R. Convery,⁶⁸ M. Cristinziani,⁶⁸ G. De Nardo,⁶⁸ D. Dong,⁶⁸ J. Dorfan,⁶⁸ D. Dujmic,⁶⁸ W. Dunwoodie,⁶⁸ E. E. Elsen,⁶⁸ S. Fan,⁶⁸ R. C. Field,⁶⁸ T. Glanzman,⁶⁸ S. J. Gowdy,⁶⁸ T. Hadig,⁶⁸ V. Halyo,⁶⁸ C. Hast,⁶⁸ T. Hryn'ova,⁶⁸ W. R. Innes,⁶⁸ M. H. Kelsey,⁶⁸ P. Kim,⁶⁸ M. L. Kocian,⁶⁸ D. W. G. S. Leith,⁶⁸ J. Libby,⁶⁸ S. Luitz,⁶⁸ V. Luth,⁶⁸ H. L. Lynch,⁶⁸ H. Marsiske,⁶⁸ R. Messner,⁶⁸ D. R. Muller,⁶⁸ C. P. O'Grady,⁶⁸ V. E. Ozcan,⁶⁸ A. Perazzo,⁶⁸ M. Perl,⁶⁸ S. Petrak,⁶⁸ B. N. Ratcliff,⁶⁸ A. Roodman,⁶⁸ A. A. Salnikov,⁶⁸ R. H. Schindler,⁶⁸ J. Schwiening,⁶⁸ G. Simi,⁶⁸ A. Snyder,⁶⁸ A. Soha,⁶⁸ J. Stelzer,⁶⁸ D. Su,⁶⁸ M. K. Sullivan,⁶⁸ J. Va'vra,⁶⁸ S. R. Wagner,⁶⁸ M. Weaver,⁶⁸ A. J. R. Weinstein,⁶⁸ W. J. Wisniewski,⁶⁸ M. Wittgen,⁶⁸ D. H. Wright,⁶⁸ A. K. Yarritu,⁶⁸ C. C. Young,⁶⁸ P. R. Burchat,⁶⁹ A. J. Edwards,⁶⁹ T. I. Meyer,⁶⁹ B. A. Petersen,⁶⁹ C. Roat,⁶⁹ S. Ahmed,⁷⁰ M. S. Alam,⁷⁰ J. A. Ernst,⁷⁰ M. A. Saeed,⁷⁰ M. Saleem,⁷⁰ F. R. Wappler,⁷⁰ W. Bugg,⁷¹ M. Krishnamurthy,⁷¹ S. M. Spanier,⁷¹ R. Eckmann,⁷² H. Kim,⁷² J. L. Ritchie,⁷² A. Satpathy,⁷² R. F. Schwitters,⁷² J. M. Izen,⁷³ I. Kitayama,⁷³ X. C. Lou,⁷³ S. Ye,⁷³ F. Bianchi,⁷⁴ M. Bona,⁷⁴ F. Gallo,⁷⁴ D. Gamba,⁷⁴ C. Borean,⁷⁵ L. Bosisio,⁷⁵ C. Cartaro,⁷⁵ F. Cossutti,⁷⁵ G. Della Ricca,⁷⁵ S. Dittongo,⁷⁵ S. Grancagnolo,⁷⁵ L. Lanceri,⁷⁵ P. Poropat,^{75,§} L. Vitale,⁷⁵ G. Vuagnin,⁷⁵ R. S. Panvini,⁷⁶ Sw. Banerjee,⁷⁷ C. M. Brown,⁷⁷ D. Fortin,⁷⁷ P. D. Jackson,⁷⁷ R. Kowalewski,⁷⁷ J. M. Roney,⁷⁷ H. R. Band,⁷⁸ S. Dasu,⁷⁸ M. Datta,⁷⁸ A. M. Eichenbaum,⁷⁸ M. Graham,⁷⁸ J. J. Hollar,⁷⁸ J. R. Johnson,⁷⁸ P. E. Kutter,⁷⁸ H. Li,⁷⁸ R. Liu,⁷⁸ A. Mihalyi,⁷⁸ A. K. Mohapatra,⁷⁸ Y. Pan,⁷⁸ R. Prepost,⁷⁸ A. E. Rubin,⁷⁸ S. J. Sekula,⁷⁸ P. Tan,⁷⁸ J. H. von Wimmersperg-Toeller,⁷⁸ J. Wu,⁷⁸ S. L. Wu,⁷⁸ Z. Yu,⁷⁸ M. G. Greene,⁷⁹ and H. Neal⁷⁹

(The BABAR Collaboration)

¹Laboratoire de Physique des Particules, F-74941 Annecy-le-Vieux, France

²Università di Bari, Dipartimento di Fisica and INFN, I-70126 Bari, Italy

³Institute of High Energy Physics, Beijing 100039, China

⁴University of Bergen, Inst. of Physics, N-5007 Bergen, Norway

⁵Lawrence Berkeley National Laboratory and University of California, Berkeley, CA 94720, USA

⁶University of Birmingham, Birmingham, B15 2TT, United Kingdom

⁷Ruhr Universität Bochum, Institut für Experimentalphysik 1, D-44780 Bochum, Germany

⁸University of Bristol, Bristol BS8 1TL, United Kingdom

⁹University of British Columbia, Vancouver, BC, Canada V6T 1Z1

¹⁰Brunel University, Uxbridge, Middlesex UB8 3PH, United Kingdom

¹¹Budker Institute of Nuclear Physics, Novosibirsk 630090, Russia

¹²University of California at Irvine, Irvine, CA 92697, USA

¹³University of California at Los Angeles, Los Angeles, CA 90024, USA

¹⁴University of California at Riverside, Riverside, CA 92521, USA

¹⁵University of California at San Diego, La Jolla, CA 92093, USA

¹⁶University of California at Santa Barbara, Santa Barbara, CA 93106, USA

¹⁷University of California at Santa Cruz, Institute for Particle Physics, Santa Cruz, CA 95064, USA

¹⁸California Institute of Technology, Pasadena, CA 91125, USA

¹⁹University of Cincinnati, Cincinnati, OH 45221, USA

- ²⁰ University of Colorado, Boulder, CO 80309, USA
- ²¹ Colorado State University, Fort Collins, CO 80523, USA
- ²² Technische Universität Dresden, Institut für Kern- und Teilchenphysik, D-01062 Dresden, Germany
- ²³ Ecole Polytechnique, LLR, F-91128 Palaiseau, France
- ²⁴ University of Edinburgh, Edinburgh EH9 3JZ, United Kingdom
- ²⁵ Università di Ferrara, Dipartimento di Fisica and INFN, I-44100 Ferrara, Italy
- ²⁶ Florida A&M University, Tallahassee, FL 32307, USA
- ²⁷ Laboratori Nazionali di Frascati dell'INFN, I-00044 Frascati, Italy
- ²⁸ Università di Genova, Dipartimento di Fisica and INFN, I-16146 Genova, Italy
- ²⁹ Harvard University, Cambridge, MA 02138, USA
- ³⁰ Universität Heidelberg, Physikalisches Institut, Philosophenweg 12, D-69120 Heidelberg, Germany
- ³¹ Imperial College London, London, SW7 2AZ, United Kingdom
- ³² University of Iowa, Iowa City, IA 52242, USA
- ³³ Iowa State University, Ames, IA 50011-3160, USA
- ³⁴ Laboratoire de l'Accélérateur Linéaire, F-91898 Orsay, France
- ³⁵ Lawrence Livermore National Laboratory, Livermore, CA 94550, USA
- ³⁶ University of Liverpool, Liverpool L69 7ZE, United Kingdom
- ³⁷ Queen Mary, University of London, E1 4NS, United Kingdom
- ³⁸ University of London, Royal Holloway and Bedford New College, Egham, Surrey TW20 0EX, United Kingdom
- ³⁹ University of Louisville, Louisville, KY 40292, USA
- ⁴⁰ University of Manchester, Manchester M13 9PL, United Kingdom
- ⁴¹ University of Maryland, College Park, MD 20742, USA
- ⁴² University of Massachusetts, Amherst, MA 01003, USA
- ⁴³ Massachusetts Institute of Technology, Laboratory for Nuclear Science, Cambridge, MA 02139, USA
- ⁴⁴ McGill University, Montréal, QC, Canada H3A 2T8
- ⁴⁵ Università di Milano, Dipartimento di Fisica and INFN, I-20133 Milano, Italy
- ⁴⁶ University of Mississippi, University, MS 38677, USA
- ⁴⁷ Université de Montréal, Laboratoire René J. A. Lévesque, Montréal, QC, Canada H3C 3J7
- ⁴⁸ Mount Holyoke College, South Hadley, MA 01075, USA
- ⁴⁹ Università di Napoli Federico II, Dipartimento di Scienze Fisiche and INFN, I-80126, Napoli, Italy
- ⁵⁰ NIKHEF, National Institute for Nuclear Physics and High Energy Physics, NL-1009 DB Amsterdam, The Netherlands
- ⁵¹ University of Notre Dame, Notre Dame, IN 46556, USA
- ⁵² Oak Ridge National Laboratory, Oak Ridge, TN 37831, USA
- ⁵³ Ohio State University, Columbus, OH 43210, USA
- ⁵⁴ University of Oregon, Eugene, OR 97403, USA
- ⁵⁵ Università di Padova, Dipartimento di Fisica and INFN, I-35131 Padova, Italy
- ⁵⁶ Universités Paris VI et VII, Lab de Physique Nucléaire H. E., F-75252 Paris, France
- ⁵⁷ Università di Pavia, Dipartimento di Elettronica and INFN, I-27100 Pavia, Italy
- ⁵⁸ University of Pennsylvania, Philadelphia, PA 19104, USA
- ⁵⁹ Università di Perugia, Dipartimento di Fisica and INFN, I-06100 Perugia, Italy
- ⁶⁰ Università di Pisa, Dipartimento di Fisica, Scuola Normale Superiore and INFN, I-56127 Pisa, Italy
- ⁶¹ Prairie View A&M University, Prairie View, TX 77446, USA
- ⁶² Princeton University, Princeton, NJ 08544, USA
- ⁶³ Università di Roma La Sapienza, Dipartimento di Fisica and INFN, I-00185 Roma, Italy
- ⁶⁴ Universität Rostock, D-18051 Rostock, Germany
- ⁶⁵ Rutherford Appleton Laboratory, Chilton, Didcot, Oxon, OX11 0QX, United Kingdom
- ⁶⁶ DSM/Dapnia, CEA/Saclay, F-91191 Gif-sur-Yvette, France
- ⁶⁷ University of South Carolina, Columbia, SC 29208, USA
- ⁶⁸ Stanford Linear Accelerator Center, Stanford, CA 94309, USA
- ⁶⁹ Stanford University, Stanford, CA 94305-4060, USA
- ⁷⁰ State Univ. of New York, Albany, NY 12222, USA
- ⁷¹ University of Tennessee, Knoxville, TN 37996, USA
- ⁷² University of Texas at Austin, Austin, TX 78712, USA
- ⁷³ University of Texas at Dallas, Richardson, TX 75083, USA
- ⁷⁴ Università di Torino, Dipartimento di Fisica Sperimentale and INFN, I-10125 Torino, Italy
- ⁷⁵ Università di Trieste, Dipartimento di Fisica and INFN, I-34127 Trieste, Italy
- ⁷⁶ Vanderbilt University, Nashville, TN 37235, USA
- ⁷⁷ University of Victoria, Victoria, BC, Canada V8W 3P6
- ⁷⁸ University of Wisconsin, Madison, WI 53706, USA
- ⁷⁹ Yale University, New Haven, CT 06511, USA

(Dated: November 3, 2018)

We establish upper limits on branching fractions for B^0 decays to final states where the decay products are purely invisible (*i.e.*, no observable final state particles) and for B^0 decays to $\nu\bar{\nu}\gamma$.

Within the Standard Model, these decays have branching fractions that are below current experimental sensitivity, but various models of physics beyond the Standard Model predict significant contributions from these channels. Using 88.5 million $B\bar{B}$ pairs collected at the $\Upsilon(4S)$ resonance by the BABAR experiment at the PEP-II e^+e^- storage ring at the Stanford Linear Accelerator Center, we establish upper limits at the 90% confidence level of 22×10^{-5} for the branching fraction of $B^0 \rightarrow$ invisible and 4.7×10^{-5} for the branching fraction of $B^0 \rightarrow \nu\bar{\nu}\gamma$.

PACS numbers: 13.20.He,12.15.Ji,12.60.Jv

This paper describes a novel search for “disappearance decays” of B^0 mesons [1], where the B^0 decay contains no observable final state particles, or such “invisible” decay products plus a single photon. Invisible decay products are particles that are neither charged nor would generate a signal in an electromagnetic calorimeter. These include neutrinos, as well as exotic, hypothetical particles (such as neutralinos). The rate for invisible B decays is negligibly small within the Standard Model (SM) of particle physics, but can be larger in several models of new physics. The SM decay $B^0 \rightarrow \nu\bar{\nu}$, which would give such an invisible experimental signature, is strongly helicity-suppressed by a factor of order $(m_\nu/m_{B^0})^2$ [2]. When combined with the weak coupling constant G_F^2 , the resulting branching fraction is necessarily well below the range of present experimental observability. The SM expectation for the $B^0 \rightarrow \nu\bar{\nu}\gamma$ branching fraction is predicted to be of order 10^{-9} , with very little hadronic uncertainty [3]. An experimental observation of an invisible ($+\gamma$) decay of a B^0 with current experimental sensitivity would thus be a clear sign of beyond-SM physics, as it could not be accommodated within SM theoretical uncertainty. No quantitative experimental bounds on B^0 to invisible or $\nu\bar{\nu}\gamma$ have been previously established; however, a reinterpretation of data used for previous constraints on $b \rightarrow s\nu\bar{\nu}$ and other modes could potentially imply upper limits on the quark-level process of this decay [4].

Several models of new physics can give significant branching fractions for invisible decays of the B^0 . A phenomenological model motivated by the observation of an anomalous number of dimuon events by the NuTeV experiment allows for an invisible B^0 decay to a $\bar{\nu}\chi_1^0$ final state, where χ_1^0 is a neutralino, with a branching fraction in the 10^{-7} to 10^{-6} range [5, 6]. Also, models with large extra dimensions, which would provide a possible solution to the hierarchy problem, can also have the effect of producing significant, although small, rates for invisible B^0 decays [7, 8, 9].

The data used in this analysis were collected with the BABAR detector at the PEP-II e^+e^- collider. The data sample consists of an integrated luminosity of 81.5 fb^{-1} accumulated at the $\Upsilon(4S)$ resonance, containing (88.5 ± 1.0) million $B\bar{B}$ pair events, and 9.6 fb^{-1} accumulated at a center-of-mass (CM) energy about 30 MeV below $B\bar{B}$ threshold. The asymmetric energies of the PEP-II e^+ and e^- beams result in a Lorentz boost $\beta\gamma \approx 0.55$ of

the $B\bar{B}$ pairs.

A detailed description of the BABAR detector is presented in Ref. [10]. Charged particle momenta are measured in a tracking system consisting of a 5-layer double-sided silicon vertex tracker (SVT) and a 40-layer hexagonal-cell wire drift chamber (DCH). The SVT and DCH operate within a 1.5 T solenoidal field, and have a combined solid angle coverage in the CM frame of 90.5%. Photons and long-lived neutral hadrons are detected and their energies are measured in a CsI(Tl) electromagnetic calorimeter (EMC), which has a solid angle coverage in the CM frame of 90.9%. Muons are identified in the instrumented flux return (IFR), composed of resistive plate chambers and layers of iron that return the magnetic flux of the solenoid. A detector of internally reflected Cherenkov light (DIRC) is used for identification of charged kaons and pions. A GEANT4 [11] based Monte Carlo simulation of the BABAR detector response was used to optimize the signal selection criteria and evaluate the signal detection efficiency.

The detection of invisible B decays uses the fact that B mesons are created in pairs, due to flavor conservation in e^+e^- interactions. If one B is reconstructed in an event, one can thus infer that another B has been produced. This technique has been exploited in several BABAR analyses [12, 13, 14]. We reconstruct events in which a B^0 decays to $D^{(*)-}\ell^+\nu$, then look for consistency with an invisible decay of the other neutral B (no observable final state particles) in the rest of the event. In order to help reject non- $B\bar{B}$ background, R2, the ratio of the second and zeroth Fox-Wolfram moments, is required to be less than 0.5 [15].

We reconstruct $D^{(*)-}$ in the decay modes $D^- \rightarrow K^+\pi^-\pi^-$ and $D^{*-} \rightarrow \bar{D}^0\pi^-$ where, in the latter case, \bar{D}^0 is reconstructed in the decay modes $K^+\pi^-$, $K^+\pi^-\pi^0$, or $K^+\pi^-\pi^+\pi^-$. To form $D^{(*)-}$ candidates in these decay modes, K^+ candidates are combined with other tracks and π^0 candidates in the event. We identify K^+ candidates using Cherenkov-light information from the DIRC and energy-loss information (dE/dx) from the DCH and SVT. The π^0 candidates are composed of pairs of photons in the EMC. Each photon must have a reconstructed energy above 30 MeV in the laboratory frame, and the sum of their energies must be greater than 200 MeV. The π^0 candidates must have an invariant mass between 115 and 150 MeV/c^2 . A mass-constrained fit is imposed on π^0 candidates in order to improve the resolution on the

reconstructed invariant mass of the parent D meson.

We require the \bar{D}^0 and D^- candidates to have reconstructed invariant masses within 20 MeV/c^2 of their respective nominal masses [16], except for \bar{D}^0 decays with a π^0 daughter, which must be within 35 MeV/c^2 of the nominal \bar{D}^0 mass. Mass-constrained fits are applied to \bar{D}^0 and D^- candidates in order to improve the measurement of the momentum of each D . The difference in reconstructed mass between D^{*-} decay candidates and their \bar{D}^0 daughters must be less than 150 MeV/c^2 . All D^{*-} candidates must have a total momentum between 0.5 and 2.5 GeV/c in the CM frame.

Tracks selected as lepton candidates must pass either electron or muon selection criteria. We identify electron candidates using energy and cluster shape information from the EMC, and Cherenkov angle information from the DIRC. Muon candidates are identified using information from the IFR and EMC. Both electrons and muons must also have a momentum of at least 1 GeV/c , and a minimum of 20 DCH measurements.

To select $B^0 \rightarrow D^{*-}\ell^+\nu$ candidates, we require a D^{*-} candidate and a lepton candidate to be consistent with production at a common point in space. We then calculate the cosine of the angle between the $D^{*-}\ell^+$ and the hypothesized B^0 candidate, under the assumption that the only particle missing is a neutrino:

$$\cos\theta_{B,D^{*-}\ell^+} = \frac{(2E_B E_{D^{*-}\ell^+} - m_B^2 - m_{D^{*-}\ell^+}^2)}{2|\vec{p}_B||\vec{p}_{D^{*-}\ell^+}|}. \quad (1)$$

The energy $E_{D^{*-}\ell^+}$ and mass $m_{D^{*-}\ell^+}$ of the $D^{*-}\ell^+$ combination are determined from reconstructed momentum information, and m_B is the nominal B^0 mass. The B^0 momentum $|\vec{p}_B|$ and energy E_B are determined from beam parameters. When the assumption that a neutrino is the only missing particle is incorrect, $\cos\theta_{B,D^{*-}\ell^+}$ can fall outside the region $[-1, 1]$. We thus require the $D^{*-}\ell^+$ combination to satisfy $-2.5 < \cos\theta_{B,D^{*-}\ell^+} < 1.1$. The asymmetric cut admits higher mass D^* states where the additional decay products are lost, and allows for detector energy and momentum resolution. When more than one such $D^{*-}\ell^+$ candidate is reconstructed in an event, the one with the smallest value of $|\cos\theta_{B,D^{*-}\ell^+}|$ is taken. We reconstruct a total of 126108 $B^0 \rightarrow D^{*-}\ell^+\nu$ candidate events in the data sample, with a purity of approximately 66%.

We consider events with no charged tracks besides those of a $B^0 \rightarrow D^{*-}\ell^+\nu$ candidate. Removing all decay products of the $D^{*-}\ell^+\nu$ candidate from consideration, we count the number of remaining EMC clusters consistent with a K_L^0 hypothesis, $N_{K_L^0}^{\text{extra}}$, and with a photon hypothesis, N_γ^{extra} . Due to accelerator-induced background and detector noise, the optimal requirements on $N_{K_L^0}^{\text{extra}}$ and N_γ^{extra} are loose. For $B^0 \rightarrow \text{invisible}$ candidates, we require that $N_{K_L^0}^{\text{extra}} < 3$ and $N_\gamma^{\text{extra}} < 3$. For $B^0 \rightarrow \nu\bar{\nu}\gamma$ candidates, we require only that there be one

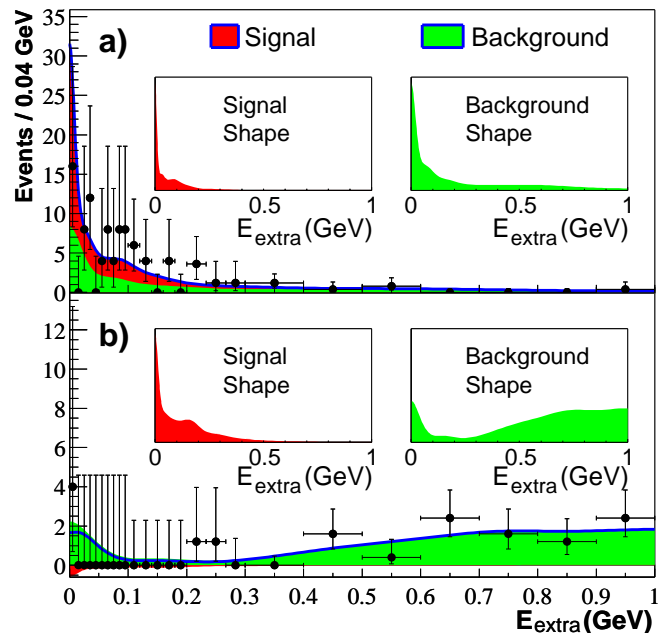


FIG. 1: Distributions of E_{extra} for (a) $B^0 \rightarrow \text{invisible}$ and (b) $B^0 \rightarrow \nu\bar{\nu}\gamma$. The points with error bars correspond to data. The curves represent maximum likelihood fits to a sum of distributions modelling signal and background.

remaining photon candidate with energy greater than 1.2 GeV in the CM frame.

The total energy in the EMC, in the CM frame, of photon clusters that remain after the decay products of the $D^{*-}\ell^+\nu$ candidate are removed, is denoted by E_{extra} . For $B^0 \rightarrow \nu\bar{\nu}\gamma$, the energy of the highest-energy photon remaining in the event (the hypothesized signal photon) is also removed from E_{extra} . In both $B^0 \rightarrow \text{invisible}$ and $B^0 \rightarrow \nu\bar{\nu}\gamma$, this variable is strongly peaked near zero for signal, whereas for the background it is less strongly peaked, as seen in Fig. 1. The background can peak near zero due to events in which all charged and neutral particles from the signal B^0 are either outside the fiducial volume of the detector, or are unreconstructed. For $B^0 \rightarrow \nu\bar{\nu}\gamma$, the background shape increases at large E_{extra} due to photons arising from misreconstructed π^0 decays, and the best-fit amount of signal is slightly (but not significantly) negative. We construct probability density functions (PDFs) for the E_{extra} distribution for signal (\mathcal{F}_{sig}) and background ($\mathcal{F}_{\text{bkgd}}$) using detailed simulation of signal and background data. The background from accelerator and detector noise is modelled using randomly-triggered events in data. The two PDFs are combined into an extended maximum likelihood function \mathcal{L} , defined

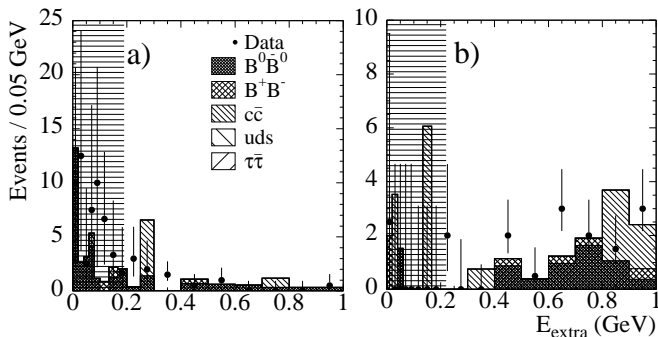


FIG. 2: Comparison of E_{extra} between data (points with error bars) and Monte Carlo background simulation (histograms) for (a) $B^0 \rightarrow \text{invisible}$ and (b) $B^0 \rightarrow \nu\bar{\nu}\gamma$. The multiple categories of background in the detector ($\Upsilon(4S) \rightarrow B^0\bar{B}^0$; $\Upsilon(4S) \rightarrow B^+B^-$; $e^+e^- \rightarrow c\bar{c}$; $e^+e^- \rightarrow u\bar{u}, d\bar{d},$ or $s\bar{s}$; and $e^+e^- \rightarrow \tau^+\tau^-$ events) are each simulated by the Monte Carlo and plotted cumulatively. No background from $e^+e^- \rightarrow u\bar{u}, d\bar{d}, s\bar{s},$ or $\tau^+\tau^-$ is seen in the Monte Carlo sample. For both of the modes, signal would tend to peak strongly in the horizontally-shaded region.

as a function of the free parameters N_{sig} and N_{bkgd}

$$\mathcal{L}(N_{\text{sig}}, N_{\text{bkgd}}) = \frac{e^{-(N_{\text{sig}}+N_{\text{bkgd}})}}{N!} \times \prod_{i=1}^N (N_{\text{sig}}\mathcal{F}_{\text{sig}}(E_i) + N_{\text{bkgd}}\mathcal{F}_{\text{bkgd}}(E_i)), \quad (2)$$

where N_{sig} and N_{bkgd} are the number of signal and background events, respectively. The fixed parameters N and E_i are the total number of events in the data sample and the value of E_{extra} for the i th event, respectively. The negative log-likelihood ($-\ln\mathcal{L}$) is then minimized with respect to N_{sig} and N_{bkgd} in the data sample. The resulting fitted values of N_{sig} and N_{bkgd} are 17 ± 9 and 19_{-8}^{+10} for $B^0 \rightarrow \text{invisible}$ and $-1.1_{-1.9}^{+2.4}$ and 28_{-5}^{+6} for $B^0 \rightarrow \nu\bar{\nu}\gamma$, where the errors are statistical. Figure 2 shows the E_{extra} distributions for $B^0 \rightarrow \text{invisible}$ and $B^0 \rightarrow \nu\bar{\nu}\gamma$.

Using detailed Monte Carlo simulation of $B^0 \rightarrow \text{invisible}$ and $\nu\bar{\nu}\gamma$ events, we determine our signal efficiency to be $(16.7 \pm 1.0) \times 10^{-4}$ for $B^0 \rightarrow \text{invisible}$ and $(14.4 \pm 1.0) \times 10^{-4}$ for $B^0 \rightarrow \nu\bar{\nu}\gamma$, where the errors are again statistical. For the $B^0 \rightarrow \nu\bar{\nu}\gamma$ channel, we assume a photon momentum distribution predicted by the constituent quark model for $B^0 \rightarrow \nu\bar{\nu}\gamma$ decay, as given in Ref. [3]. Of signal events that contain a reconstructed $B^0 \rightarrow D^{(*)-}\ell^+\nu$, approximately 46% (30%) of $B^0 \rightarrow \text{invisible}$ ($B^0 \rightarrow \nu\bar{\nu}\gamma$) events pass the signal selection.

We consider systematic uncertainties on the signal reconstruction efficiency, and also the uncertainty on the ratio of background to signal determined in the fit. Systematic uncertainties on the signal efficiency are dominated by the statistical size of the signal Monte Carlo

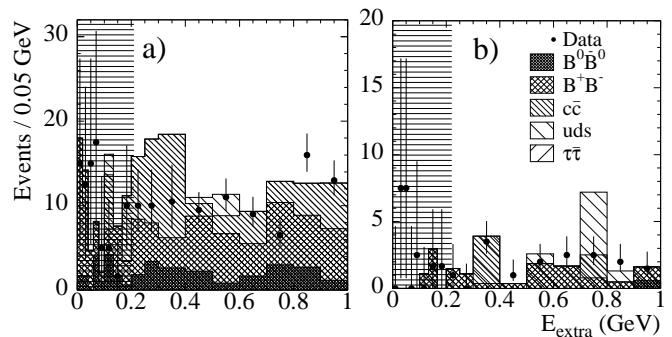


FIG. 3: Comparison of E_{extra} between data (points with error bars) and Monte Carlo background simulation (histograms) for the validation channels (a) $B^\pm \rightarrow \text{invisible}$ and (b) $B^\pm \rightarrow \nu\bar{\nu}\gamma$. No background from $e^+e^- \rightarrow \tau^+\tau^-$ is seen in the Monte Carlo sample.

sample (resulting in relative uncertainties of 6.5% and 6.8% for $B^0 \rightarrow \text{invisible}$ and $B^0 \rightarrow \nu\bar{\nu}\gamma$, respectively) and by uncertainty on the efficiency for determining the particle type of charged tracks (5.4% for both channels). Systematic uncertainty on the number of signal events, due to uncertainty on the ratio of background to signal in the fit, is dominated by the parametrization of the background and signal shapes (resulting in uncertainties on the number of signal events of 6.1 and 0.5 events for $B^0 \rightarrow \text{invisible}$ and $B^0 \rightarrow \nu\bar{\nu}\gamma$, respectively) and by the energy resolution for reconstructing neutral clusters in the EMC (3.2 and 3.4 events, respectively). Other systematic uncertainties include the efficiency for reconstructing the charged tracks in the $B^0 \rightarrow D^{(*)-}\ell^+\nu$ decay, the charged track momentum resolution, and the total number of $B\bar{B}$ events in the data sample. The total systematic uncertainties on the efficiency are 10.9% and 11.1%, and on the fitted number of signal events are 7.4 and 4.3 events, for $B^0 \rightarrow \text{invisible}$ and $B^0 \rightarrow \nu\bar{\nu}\gamma$, respectively.

To determine 90% confidence level (C.L.) upper limits on the branching fractions of $B^0 \rightarrow \text{invisible}$ and $B^0 \rightarrow \nu\bar{\nu}\gamma$, we generate 8000 Monte Carlo experiments, each parametrized by the fitted numbers of signal and background events, the efficiency, and the number of $B\bar{B}$ events in the data sample. Errors are incorporated into the simulated experiments via a convolution of the systematic effects (treated as Gaussian distributions) and the statistical error (taken from the non-Gaussian likelihood function from the fit).

The resulting upper limits on the branching fractions are

$$\mathcal{B}(B^0 \rightarrow \text{invisible}) < 22 \times 10^{-5} \text{ and} \\ \mathcal{B}(B^0 \rightarrow \nu\bar{\nu}\gamma) < 4.7 \times 10^{-5} \text{ at 90\% C.L.}$$

If the $B^0 \rightarrow \text{invisible}$ branching fraction were zero, the probability of observing an equal or larger signal yield would be 6%.

We perform validation cross-checks on the results of this analysis. To check the measurement of the efficiency for reconstructing $B^0 \rightarrow D^{(*)-}\ell^+\nu$ decays (which was determined using Monte Carlo simulation), we select a data sample in which a B^0 and a \bar{B}^0 are both reconstructed as decays to $D^{(*)}\ell\nu$ in the same event. Using the ratio of such “double tag” data events to events where just a single $D^{(*)}\ell\nu$ is reconstructed, and the number of $B^0\bar{B}^0$ events in the full data sample, we determine the efficiency for $B^0 \rightarrow D^{(*)-}\ell^+\nu$ reconstruction in data. The result is consistent with that obtained from Monte Carlo simulation.

We also search for the unphysical modes $B^\pm \rightarrow$ invisible and $B^\pm \rightarrow \nu\bar{\nu}\gamma$ (which would violate charge conservation), to check that their resulting signal is consistent with zero. For these modes, we reconstruct $B^\pm \rightarrow D^0\ell\nu X^0$, where X^0 can be a photon, π^0 , or nothing. The D^0 is reconstructed in the same three decay modes as in $B^0 \rightarrow D^{(*)-}\ell^+\nu$, and similar criteria are enforced for the reconstructed B as for the neutral B modes. All systematic errors are considered, and the “double tags” validation above is also performed for B^\pm reconstruction. The resulting fitted values of N_{sig} are $-6_{-9}^{+10}(\text{stat.})\pm 6(\text{syst.})$ for $B^\pm \rightarrow$ invisible and $8_{-4}^{+5}(\text{stat.})\pm 4(\text{syst.})$ for $B^\pm \rightarrow \nu\bar{\nu}\gamma$, which are both consistent with zero. Figure 3 shows the E_{extra} distributions for the two validation modes.

In summary, we obtain limits on branching fractions for B^0 decays to an invisible final state and for B^0 decays to $\nu\bar{\nu}\gamma$. The upper limits at 90% confidence level are 22×10^{-5} and 4.7×10^{-5} for the $B^0 \rightarrow$ invisible and $B^0 \rightarrow \nu\bar{\nu}\gamma$ branching fractions, respectively. The latter limit assumes a photon momentum distribution predicted by the constituent quark model for $B^0 \rightarrow \nu\bar{\nu}\gamma$ decay [3], whereas the $B^0 \rightarrow$ invisible limit is not decay-model dependent.

We are grateful for the excellent luminosity and machine conditions provided by our PEP-II colleagues, and for the substantial dedicated effort from the computing organizations that support BABAR. The collaborating institutions wish to thank SLAC for its support and kind hospitality. This work is supported by DOE and NSF (USA), NSERC (Canada), IHEP (China), CEA and

CNRS-IN2P3 (France), BMBF and DFG (Germany), INFN (Italy), FOM (The Netherlands), NFR (Norway), MIST (Russia), and PPARC (United Kingdom). Individuals have received support from the A. P. Sloan Foundation, Research Corporation, and Alexander von Humboldt Foundation.

* Now at Department of Physics, University of Warwick, Coventry, United Kingdom

† Also with Università della Basilicata, Potenza, Italy

‡ Also with IFIC, Instituto de Física Corpuscular, CSIC-Universidad de Valencia, Valencia, Spain

§ Deceased

- [1] Charge-conjugate decay modes are implied throughout this paper.
- [2] G. Buchalla and A.J. Buras, Nucl. Phys. **B 400**, 225 (1993).
- [3] C.D. Lu and D.X. Zhang, Phys. Lett. **B 381**, 348 (1996).
- [4] ALEPH Collaboration, R. Barate *et al.*, Eur. Phys. Jour. **C 19**, 213 (2001).
- [5] NuTeV Collaboration, T. Adams *et al.*, Phys. Rev. Lett. **87**, 041801 (2001).
- [6] A. Dedes, H. Dreiner, and P. Richardson, Phys. Rev. **D 65**, 015001 (2002).
- [7] K. Agashe, N.G. Deshpande, and G.-H. Wu, Phys. Lett. **B 489**, 367 (2000).
- [8] K. Agashe and G.-H. Wu, Phys. Lett. **B 498**, 230 (2001).
- [9] H. Davoudiasl, P. Langacker, and M. Perelstein, Phys. Rev. **D 65**, 105015 (2002).
- [10] BABAR Collaboration, B. Aubert *et al.*, Nucl. Instr. and Methods **A 479**, 1 (2002).
- [11] GEANT4 Collaboration, S. Agostinelli *et al.*, Nucl. Instr. and Methods **A 506**, 250 (2003).
- [12] BABAR Collaboration, B. Aubert *et al.*, BABAR-CONF-03/006, hep-ex/0304020.
- [13] BABAR Collaboration, B. Aubert *et al.*, BABAR-CONF-03/005, hep-ex/0303034.
- [14] BABAR Collaboration, B. Aubert *et al.*, BABAR-CONF-03/004, hep-ex/0304030.
- [15] G.C. Fox and S. Wolfram, Phys. Rev. Lett. **41**, 1581 (1978).
- [16] Particle Data Group, K. Hagiwara *et al.*, Phys. Rev. **D 66**, 010001 (2002).